A STATISTICAL TAGUCHI METHOD STUDY FOR GRAPHENE OXIDE-TITANIUM OXIDE (GO-TiO₂) THIN FILM COATING ON GLASS SUBSTRATES USING THE SPIN COATING METHOD

İbrahim Fırat BALKAYA*, Mechanical Engineering Department, Bilecik Seyh Edebali University/Institute of Graduate, Bilecik, 1055242@ogrenci.bilecik.edu.tr

(🆔 https://orcid.org/0000-0002-7674-196X)

Nevin ATALAY GENGEÇ, Department of Environmental Protection Technologies, Kocaeli University/Izmit Vocationalschool, Kocaeli, nevin.atalay@kocaeli.edu.tr

(🆔 https://orcid.org/0000-0003-0993-4398)

Harun MİNDİVAN, Mechanical Engineering Department, Bilecik Seyh Edebali University/ Institute of Graduate, Bilecik, harun.mindivan@bilecik.edu.tr

(🆔 https://orcid.org/0000-0003-3948-253X)

Abstract

In this study, the process of coating graphene oxide-titanium oxide (GO-TiO₂) composite thin films onto a glass substrate using the spin coating method was investigated using the Taguchi experimental design approach. The effects of parameters such as spin coating speed (SCR), spin coating time (SCT), dispersion amount (V), and glass substrate plasma treatment time (PLS T) on coating performance were evaluated, and the optimal coating conditions were determined. Signal-to-noise (S/N) ratios were calculated based on the equilibrium contact angles using the L16 orthogonal array experimental design. Stable and high pure water equilibrium contact angle (CA: θe) was identified as the criterion for successful coating. Characterization was performed using X-ray Diffraction (XRD), optical microscopy, Scanning Electron Microscopy (SEM), a four-point probe conductivity measurement device, and an optical contact angle measuring instrument. The optimal coating conditions were determined using the statistical Taguchi method with Pareto Analysis of Variance (Pareto ANOVA), and the effects of the control factors were analyzed. Additionally, regression analyses were conducted to assess the significance of the parameters and their alignment with the most influential factors. Validation experiments confirmed the success of the optimization.

Keywords: Graphene oxide, Titanium oxide, Thin film, Spin coating, Contact angle, Taguchi

DÖNDÜREREK KAPLAMA YÖNTEMİYLE CAM SUBSTRAT ÜZERİNE GRAFEN OKSİT-TİTANYUM OKSİT (GO-TiO₂) İNCE FİLM KAPLAMA İÇİN İSTATİKSEL TAGUCHI METODU ÇALIŞMASI

Özet

Bu çalışmada, cam substrat üzerine, döndürerek kaplama yöntemi kullanılarak, grafen oksit-titanyum oksit (GO-TiO₂) kompozit ince film kaplama süreci, Taguchi deney tasarımı yaklaşımıyla incelenmiştir. Deneylerde, kaplama performansını etkileyen döndürme hızı (SCR), döndürme süresi (SCT), dispersiyon miktarı (V) ve cam substrat plazmalama süresi (PLS T) gibi parametrelerin etkileri değerlendirilmiş ve en uygun kaplama koşulları belirlenmiştir. L16 ortogonal dizin deney tasarımı kullanılarak, denge temas açılarına dayalı sinyal/gürültü (S/N) oranları hesaplanmıştır. Kaplamanın başarı kriteri olarak kararlı ve yüksek saf su denge temas açısı (CA: θe) belirlenmiştir. Karakterizasyon işlemleri, X Işını Kırınımı (XRD), optik mikroskop, Taramalı Elektron Mikroskobu (SEM), dört problu iletkenlik ölçüm cihazı ve optik temas açısı ölçüm cihazı ile gerçekleştirilmiştir. İstatistiksel Taguchi yöntemiyle optimum kaplama şartları Pareto Varyans analizi (Pareto ANOVA) ile belirlenmiş ve kontrol faktörlerinin etkileri analiz edilmiştir. Ayrıca, regresyon analizleri yapılarak parametrelerin etkilerinin anlamlılığı değerlendirilmiş ve en etken parametrelerle olan uyumu ortaya koyulmuştur. Doğrulama deneyleri ile optimizasyonun başarılı olduğu sonucuna ulaşılmıştır.

Anahtar Kelimeler: Grafen oksit, Titanyum oksit, İnce film, Döndürerek kaplama, Temas açısı, Taguchi

1. Introduction

Graphene oxide (GO) is a derivative of graphene, enriched with oxygen-containing functional groups, exhibiting properties such as good solubility in water, high surface area, flexibility, and electrical conductivity. These features make GO an attractive material for thin film coating technologies. The applications of GO in thin film form contribute to the advancement of various technological fields [1].

GO can be chemically reduced to form highly conductive graphene, which enables the use of thin film coatings in electronic circuits [2]. GO thin films provide an ideal material for flexible electronic devices and durable sensors. These films are resistant to mechanical stress and can be used on flexible surfaces [3]. These thin films offer high-performance electrode material for energy storage devices such as supercapacitors [4]. The biocompatibility of GO and its ability to be enriched with functional groups enable its application in areas such as biosensors, drug delivery systems, and tissue engineering [5]. As a transparent and conductive material, GO has potential applications in liquid crystal displays, optical communication systems, and solar cells [6]. Additionally, due to its high surface area and functional groups, GO holds promise for environmentally friendly and antibacterial applications [7].

Titanium dioxide (TiO₂) nanoparticles serve as an effective agent in biosensor applications due to their excellent biocompatibility, specific affinity for biomolecules, and high reactivity. Owing to its high conductivity and low cost, TiO₂ has become an attractive electrode material in various forms such as nanoparticles, nanoneedles, and nanotubes [8].

The composite thin films produced by integrating GO and TiO₂ offer a combination of the strengths of both materials [9]. GO is notable for its expansive surface area, excellent conductivity, and surface functionalization potential, while TiO₂ is known for its chemical stability and high photocatalytic efficiency [10, 11]. The oxygen-containing functional groups in GO, such as -OH and -COOH, act as suitable carriers for supporting TiO₂ nanocrystals [12]. By merging GO's large surface area, electrical conductivity, and mechanical properties with the outstanding photocatalytic activity and chemical stability of TiO₂, multifunctional thin films can be developed. The photocatalytic performance of TiO₂ under UV light is enhanced when supported by GO, leading to improved overall efficiency [9]. These materials, used as thin film coatings, have great promise, especially in areas such as energy storage, environmental remediation, and biomedical technologies [13]. GO-TiO₂ thin films are particularly relevant for applications in solar cells, supercapacitors, and wearable electronics [14]. It has been observed that 3D graphene-titanium dioxide (G-TiO₂) composite electrodes outperform 3D graphene electrodes in supercapacitors, demonstrating superior rate capability and cycle stability. This performance is attributed to the hierarchical 3D porous structure and the synergistic effect between graphene and TiO₂, highlighting the potential of G-TiO₂ composites in supercapacitors [15]. Furthermore, their antibacterial properties make these materials suitable for surface coatings in biomedical devices [16].

The spin coating method involves applying a solution to a rapidly rotating surface to produce a thin and homogeneous film. This technique is commonly used, especially for coating nanoscale materials. The spin coating of GO thin films affects crucial parameters such as coating thickness, uniformity, and surface roughness [17].

Taguchi experimental design is a widely used optimization method in quality engineering. This method is employed to evaluate and optimize the effects of critical parameters in a given process. The Taguchi method utilizes orthogonal arrays to reduce the number of experiments while allowing for the determination of parameter interactions and optimal conditions [18].

The advantages of using the Taguchi method in spin coating processes include the reduction in the number of experiments, cost reduction, and minimization of process variability [19]. This method is applied in the optimization of various types of coatings [20].

Spin speed is a critical parameter that determines the thickness and uniformity of the GO thin film. The spin speed (rpm) influences the percentage of the surface covered, and this speed is dependent on the solution concentration [21]. It has been reported that higher spin speeds result in thinner coatings [22].

This study aims to successfully coat GO-TiO₂ composite films on glass substrates via spin coating method using statistical Taguchi method and to meet optimum contact angle behaviors onto surface of GO-TiO₂ composite films.

2. Materials and Methods

In this research, a dispersion was prepared through the ultrasonication technique, which was subsequently used to coat 25x75 mm glass slide substrates via the spin coating method. The X-ray diffraction (XRD) analysis of the GO-TiO₂ composite was carried out using a Panalytical Empyrean diffractometer, while its conductivity changes were examined with a four-probe conductivity measurement system (Signatone). To determine surface homogeneity and hydrophobicity, the equilibrium contact angle (θe) of deionized water (Merck) was measured using an optical contact angle device (Biolin Scientific Theta Lite). Further characterization techniques included optical microscopy (Nikon Eclipse LV150) and scanning electron microscopy (SEM) with a Zeiss SupraV40.

The study was conducted in three stages: L16 orthogonal experimental design, Pareto Variance Analysis (Pareto ANOVA), and validation. The experimental parameters were defined as Coating Speed

(Spin Rate, SCR; rpm), Spin Time (SCT; s), Dispersion Amount (V; ml), and Plasma Time (Pls T; s) (Table 1).

Taguchi's statistical design of experiment method with larger-the-better formula (1) quality characteristic was used for the response equilibrium contact angle (θe) using excel [23].

$$\frac{S}{N}ratio = -10\log\left(\frac{1}{n}\sum_{i=1}^{n}\frac{1}{y_i^2}\right) \qquad (1)$$

Pareto Variance Analysis employs the Pareto principle for data analysis and process optimization, providing a short calculation time for parametric design data analysis. Additionally, it does not require a separate ANOVA table, thus eliminating the need for Fisher's test. Due to these conveniences, it is considered more suitable for engineers and industry personnel [23].

The calculation of Pareto Variance Analysis was performed based on the S/N ratio values obtained from the factors of Spin Rate (SCR), Spin Time (SCT), Dispersion Amount (V; ml), and Plasma Time (Pls T).

Table 1. Spin coating experiment parameters and operational levels.

Process parameters	Unit	Symbol	Level			
			1	2	3	4
Spin Rate (SCR)	rpm	A	500	1000	1500	2000
Spin Coating Time (SCT)	s	B	5	10	15	20
Dispersion Volume (V)	ml	C	0,2	0,3	0,4	0,5
Plasma Time (Pls T)	s	D	5	15	25	35

3. Experimental Study

3.1. Preparation of Stable GO-TiO₂ Dispersion

The preparation of stable dispersions typically involves ultrasonication, mixing, and centrifugation steps [24]. In this study, a graphene oxide (GO) dispersion was initially prepared by adding 1 g of graphite oxide (GrO) to 500 mL of deionized water (Merck), yielding a starting concentration of 2 mg/mL. The mixture was subjected to ultrasonication at 35 kHz for 16 hours, followed by centrifugation at 3000 rpm for 30 minutes. After centrifugation, the supernatant, a stable GO dispersion with a concentration of 0.83 mg/mL, was obtained, as determined by solid content analysis.

For the preparation of stable GO-TiO₂ dispersions, a method adapted from the GO-SnO₂ formulation used by Liang et al. was employed [25]. The GO dispersion was diluted with deionized water (Merck) to a concentration of 0.8 mg/mL and ultrasonicated for 5 minutes. Then, 0.1 g of TiO₂ was added to 250 mL of this GO dispersion, followed by 1.5 hours of ultrasonication. The dispersion was subsequently centrifuged at 3000 rpm for 5

minutes, and the supernatant was collected. The concentration of the GO-TiO₂ dispersion was found to be 0.6 mg/mL based on solid content analysis. This dispersion remained stable for two weeks and was used to fabricate GO-TiO₂ surfaces. According to Liang et al., the strong interactions between TiO₂ nanocrystals and GO layers help prevent detachment during ultrasonication [26].

3.2. GO-TiO₂ Coating Study

The initial step in the coating process requires proper preparation of the glass substrate to ensure effective adhesion of the coating. To achieve this, the glass substrates were first immersed in a chromic acid bath for 30 minutes, then thoroughly rinsed with deionized water. Afterward, the substrates were dried in a vacuum oven and subjected to vacuum plasma treatment for 5 seconds.

In this study, the surfaces were fabricated using the spin coating (SC) technique on the prepared glass substrates (Figure 1).
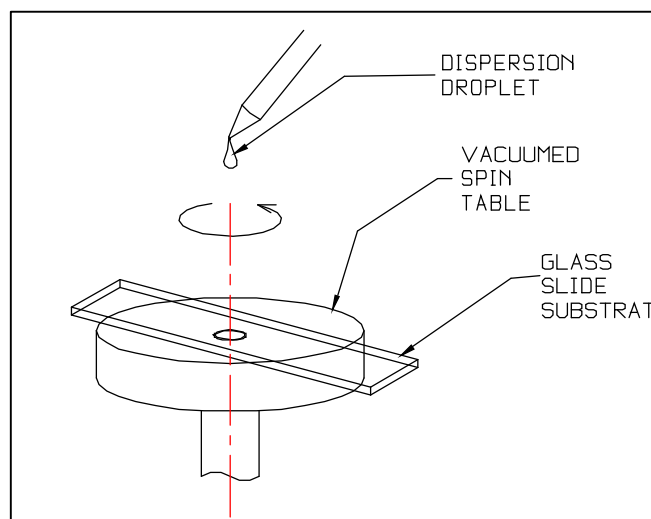

Figure 1. Schematic representation of the spin coating method.

4. Results and Discussion

4.1. Characterization Studies

The XRD analysis of the GO-TiO₂ composite (Figure 2) reveals a characteristic peak of GO at $2\theta \approx 11°$ and a peak specific to titanium at $2\theta \approx 26°$ [27, 28].

The thickness and number of layers of the GO-TiO₂ composite film were calculated from the XRD results using the Scherrer equation (Equation 2) [29] and the number of layers formula (Equation 3) [30].
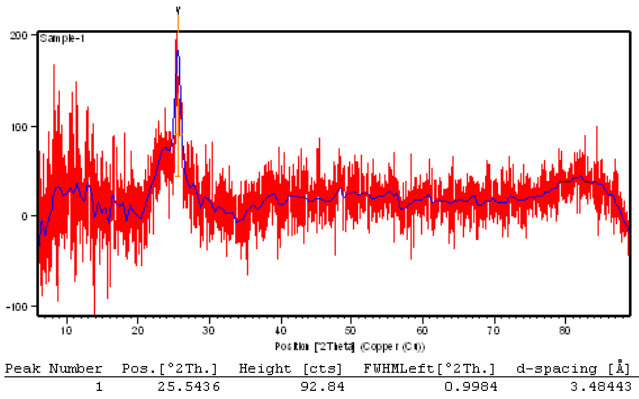
Peak Number	Pos.[°2Th.]	Height [cts]	FWHMLeft[°2Th.]	d-spacing [Å]
1	25.5436	92.84	0.9984	3.48443

Figure 2. XRD analysis of the GO-TiO₂ composite.

$$t = K.\lambda / \beta.\cos\theta \qquad (2)$$
$$N-1 = t/d \qquad (3)$$

t: Thickness of Coating; N: Number of Layer

$K=0{,}90$; $\lambda=1{,}5406$Å

β= Full-Width at Half of Max. (FWHM, rad); θ=Bragg angle.

Table 2. Calculation table of GO-TiO₂ composite thin film thickness and number of layers according to Scherrer Equation.

Surface	Pos.	d-spacing	λ	FWHM Left	t	N
	[°2Th.]	[Å]	[Å]	[°2Th.]	[μm]	
GO-TiO₂	25,5436	3,48443	1,5406	0,9984	0,00816	24

Conductivity measurements performed using a four-point probe suggest the partial formation of graphene. The surfaces of both GO solid and GO-TiO₂ solid, when exposed to the oven atmosphere, typically exhibit low conductivity. However, a comparison between the two materials reveals that the conductivity of GO-TiO₂ solid is significantly higher than that of GO solid (Table 3). This finding suggests that a reduced graphene oxide-titanium oxide (rGO-TiO₂) composite begins to form through a simple ultrasonication process, as indicated by the XRD peak at 2θ≈26°, which is characteristic of rGO-TiO₂ formation [31].

Table 3. Sheet resistance results from conductivity measurements of the solid content/precipitate of GO-deionized water and GO-TiO₂ deionized water supernatants.

Surface	Rs (ohm/sq)
GO	19328,944
GO-TiO₂	4565,932
Current (mA): 0,005	**Thickness (μm): 1**

Spin coated surface in optimum terms of TiO₂ particle adhesion and distribution on the surface, it was observed that resulted in a significantly regular distribution (Figures 3.a and 3.b).

In optimal conditions for TiO₂ particle adhesion and distribution on the spin-coated surface, it was observed that the resulting distribution was significantly uniform (Figures 3.a and 3.b).
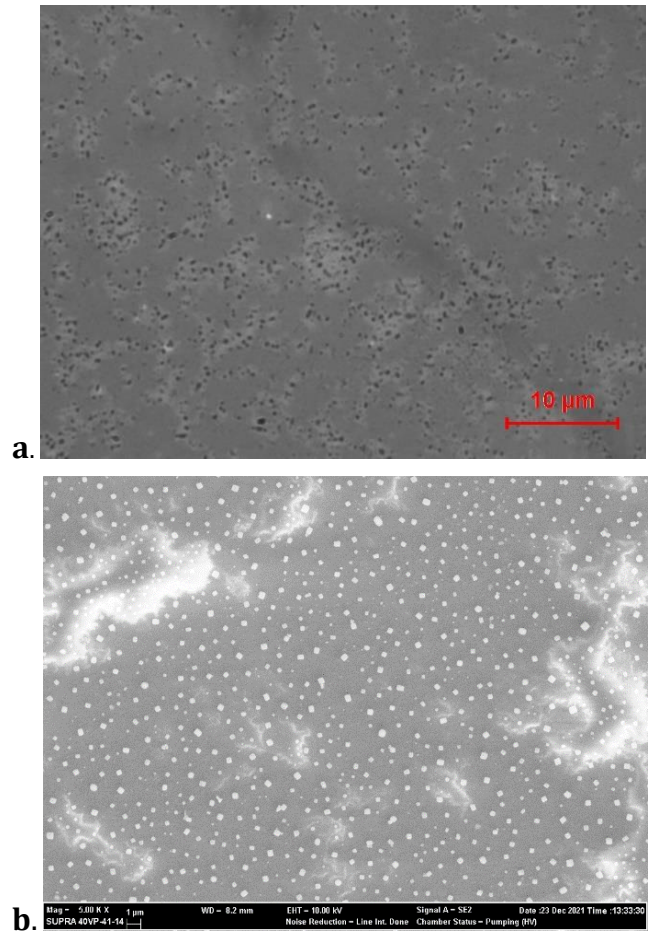

a.

b.
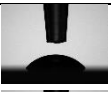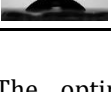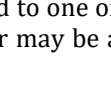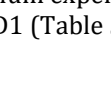
Figure 3. a. Optical microscope images (X1500), b. SEM image (X5000) of GO-TiO₂ thin film coating produced by spin (SCR=500 rpm, SCT=10s, V=0,3ml, PlsT=5s) coating method.

4.2. Experiment

In the experiment, an L16 orthogonal experimental design (Table 4) was employed. The coatings were kept in the oven at 75°C for two days and then in the desiccator for one day. For CA measurement, the average of three measurements from each coating experiment was included in the experimental design table along with drop (CA) images and S/N ratios.

Table 4. L16 orthogonal array experiment for spin coating, contact angle measurements and S/N ratios.

Exp. No	Input parameters (coded)				Input parameters (un-coded)				Average values of outputs		Average S/N ratio values of outputs
	SCR (rpm)	SCT (s)	V (ml)	PLS T (s)	SCR (rpm)	SCT (s)	ml	PLS T (s)	CA (θ)°		dB
L1	1	1	1	1	500	5	0,2	5	64°		36,12
L2	1	2	2	2	500	10	0,3	15	56°		34,96
L3	1	3	3	3	500	15	0,4	25	52°		34,32
L4	1	4	4	4	500	20	0,5	35	51°		34,15
L5	2	1	2	3	1000	5	0,3	25	52°		34,32
L6	2	2	1	4	1000	10	0,2	35	51°		34,15
L7	2	3	4	1	1000	15	0,5	5	58°		35,27
L8	2	4	3	2	1000	20	0,4	15	45°		33,06
L9	3	1	3	4	1500	5	0,4	35	39°		31,82
L10	3	2	4	3	1500	10	0,5	25	55°		34,81
L11	3	3	1	2	1500	15	0,2	15	43°		32,67
L12	3	4	2	1	1500	20	0,3	5	60°		35,56
L13	4	1	4	2	2000	5	0,5	15	43°		32,67
L14	4	2	3	1	2000	10	0,4	5	49°		33,80
L15	4	3	2	4	2000	15	0,3	35	45°		33,06
L16	4	4	1	3	2000	20	0,2	25	51°		34,15

As a result of the study, the contribution of the coating speed (SCR) to the contact angle (CA; θe) was found to be 24.894%. The dispersion amount (ml) was identified as the next major factor, contributing 17.942% to the contact angle (CA; θe). The effects of coating time (SCT) and plasma time (PLS T) were found to be 6.541% and 50.618%, respectively. The optimum experimental parameter may correspond to one of the experiments in the experimental design or may be arranged differently [32].

It was found that the optimum experimental parameters were designed as A1B2C2D1 (Table 5).

Table 5. Pareto ANOVA for contact angle responses in spin coating experiments.

Process Parameters	Levels	A	B	C	D
	1	**139,56**	134,93	137,10	**140,76**
Sums of Factor Levels	2	136,80	**137,73**	**137,91**	133,37
	3	134,86	135,32	133,01	137,60
	4	133,69	136,93	136,90	133,19
Sums of Squares of Differences		78,969	20,928	57,566	159,345
Percent Contribution Ratio (%)		24,926	6,606	18,171	50,297
Cumulative Contribution Ratio (%)		24,926	31,532	49,703	100,0
Optimal Levels		A1	B2	C2	D1
Optimal Level Parameters		SCR:500 rpm	SCT:10s	V:0,3ml	PlsT:5s

The optimal levels obtained from the Pareto ANOVA results (Table 5) are also depicted through the average signal-to-noise (S/N) ratio graphs for the factor levels (Figure 4).
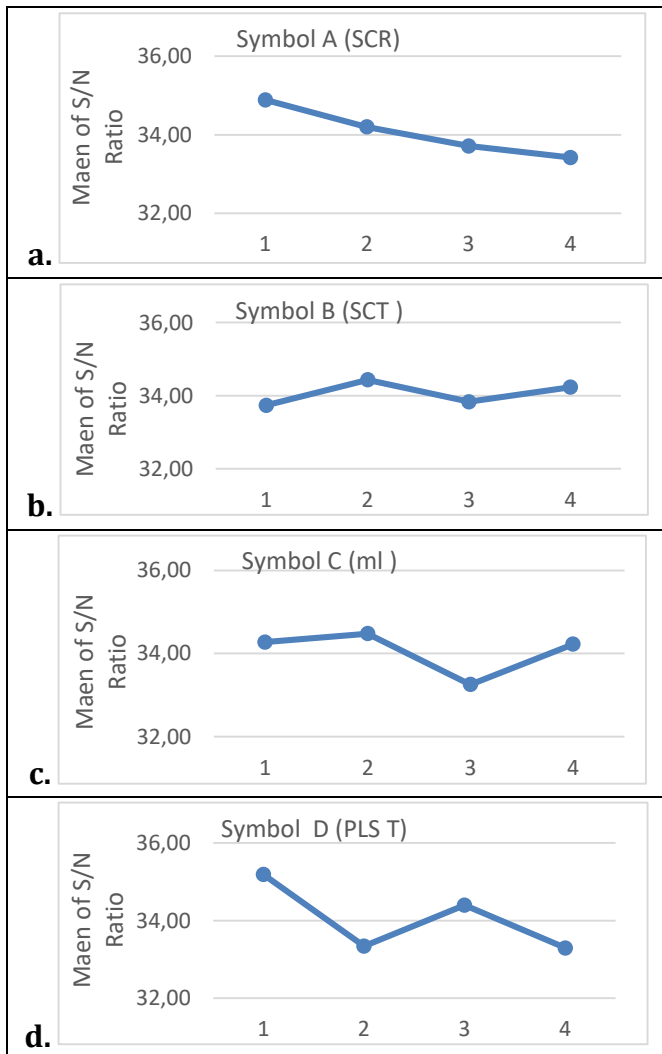

a.

b.

c.

d.

Figure 4. Average signal-to-noise (S/N) ratio graphs for the factor levels

The regression analysis results (Table 6) indicate that all variables together have a high and positive correlation of 70% with the contact angle (CA; θ), and all variables account for 49% of the total variance in the CA dimension.

Table 6. Regression statistics for the L16 experimental design coating experiment.

Multiple R	R-Squared	Standard Error	Observation
0,70	0,49	5,67	16

When examining the p-values from the regression analysis (Table 7) in the context of the effectiveness results obtained from the experimental design (Figure 4), it is evident that the plasma time (Pls T), with an effectiveness of 50.297%, and the spin rate (SCR), with the second highest effectiveness, are statistically significant ($p < 0,05$). The dispersion amount (ml), with an effectiveness of 18.171%, and the spin time (SCT), with weak effectiveness values (6.606%), do not show statistical significance ($p > 0,05$).

Table 4 shows that the highest average CA is generally observed in the experimental class with the lowest speed of 500 rpm. Additionally, in each speed group, singular maximums are obtained when the plasma time (Pls T) is set to 5 seconds. These results are consistent with the significance obtained from the regression and the Pareto ANOVA percentage contribution ratios (Table 7).

Table 7. Regression and Pareto ANOVA results for the L16 coating experiment.

	Coefficients	Standard Error	P-value	Percent Contribution Ratio (%)
Intersection	65,7000	6,94393	1,282E-06	-
SCR (rpm)	-0,0057	0,00254	0,04605	24,894
SCT (s)	0,0700	0,25356	0,78761	6,541
V (ml)	-8,5000	12,67783	0,51639	17,947
PLS T (s)	-0,2800	0,12678	0,04934	50,618

The estimated contact angle values were calculated using the regression coefficients (Table 8).

Table 8. The estimated contact angle calculation.

	Coefficient	Factor Value	Product
Constant	65,7		65,7
SCR (rpm)	-0,0057	500	-2,850
SCT (s)	0,07	10	0,700
ml	-8,5	0,300	-2,550
PLS T (s)	-0,28	5	-1,400
Estimated CA°			**59,60**

The Level D1 corresponds to the plasma time (PLS T), which is the dominant parameter with a significant contribution of 50.618% and reliability of $p<0,05$. The

values for the spin speed (SCR: 24.894%) and dispersion volume (V: 17.947%) are close to each other, and therefore, they were not included in the estimated S/N ratio calculation. The estimated S/N value was computed using Equation 4 [33].

$$\eta opt = \eta m + \sum_{i=1}^{j}(\eta i - \eta m) \qquad (4)$$

ηm : Mean S/N, ηi : Mean S/N of optimum Levels of the most effective Factor(s).

$$\eta opt = 34,06 + (35,19 - 34,06) = 35,19 \, (dB)$$

The results of the validation experiments indicate that the optimization was successful. The estimated and experimental S/N ratios, as well as the contact angles, show a high degree of consistency (Table 8).

Table 8. Verification experiment results and contact angles.

Performance Criteria	Optimum Process Parameters	
	Estimated	**Experimental**
Level	A1B2C2D1	A1B2C2D1
Contact Angle (CA; θe. °)	59,6	61,33
S/N (dB)	35,19	35,75

Bera et al., measured a contact angle of 56° for GO coatings on glass [34]. In comparison, the contact angles obtained in the recent coating experiments were approximately 61°, which is consistent with the literature and demonstrates a relative improvement.

The validation experiments were conducted to confirm the success of the optimization process. The experimental results revealed that the predicted and actual signal-to-noise (S/N) ratios and contact angles showed a high degree of agreement. This alignment indicates that the optimization process was effective and the desired film properties were achieved.

5. Results

Taguchi experimental design was used to determine the optimal combination of parameters such as spin speed, spin time, dispersion amount, and substrate plasma treatment time. This optimization has facilitated the achievement of films with desired properties in GO-TiO₂ thin film coating processes.

The most influential parameter in the coating process, with a contribution of 50.618% and a reliability of $p<0.05$, was found to be the plasma treatment time (PLS T). The second major factor meeting the reliability condition ($p<0.05$) was determined to be spin speed (SCR), with a contribution of 24.894%.

The use of ultrasonication in the addition of TiO₂ to the GO dispersion led to some degree of graphene formation, resulting in increased conductivity.

In the spin coating method, TiO₂ particles adhered to the surface with a very homogeneous distribution, achieving a very fine coating performance.

The studies conducted using the Taguchi method have demonstrated that this approach provides significant contributions to increasing efficiency in coating processes and improving material properties.

6. Acknowledgment

7. References

[1] Dreyer, D. R., Park, S., Bielawski, C. W., & Ruoff, R. S. (2010). The chemistry of graphene oxide. Chemical Society Reviews, 39(1), 228-240.

[2] Stankovich, S., Dikin, D. A., Dommett, G. H. B., Kohlhaas, K. M., Zimney, E. J., Stach, E. A., ... & Ruoff, R. S. (2006). Graphene-based composite materials. Nature, 442(7100), 282-286.

[3] Kim, H., Abdala, A. A., & Macosko, C. W. (2010). Graphene/polymer nanocomposites. Macromolecules, 43(16), 6515-6530.

[4] Xu, Y., Sheng, K., Li, C., & Shi, G. (2010). Self-assembled graphene hydrogel via a one-step hydrothermal process. ACS nano, 4(7), 4324-4330.

[5] Yang, X., Zhang, X., Ma, Y., Huang, Y., Wang, Y., & Chen, Y. (2009). Superparamagnetic graphene oxide–Fe 3 O 4 nanoparticles hybrid for controlled targeted drug carriers. Journal of materials chemistry, 19(18), 2710-2714.

[6] Becerril, H. A., Mao, J., Liu, Z., Stoltenberg, R. M., Bao, Z., & Chen, Y. (2008). Evaluation of solution-processed reduced graphene oxide films as transparent conductors. ACS Nano, 2(3), 463-470.

[7] Hu, W., Peng, C., Luo, W., Lv, M., Li, X., Li, D., ... & Fan, C. (2010). Graphene-based antibacterial paper. ACS Nano, 4(7), 4317-4323.

[8] Ensafi, A. A., Sohrabi, M., Jafari-Asl, M., & Rezaei, B. (2015). Selective and sensitive furazolidone biosensor based on DNA-modified TiO_2-reduced graphene oxide. Applied Surface Science, 356, 301-307

[9] Liu, X., Chen, C., Chen, X. A., Qian, G., Wang, J., Wang, C., ... & Liu, Q. (2018). WO3 QDs enhanced photocatalytic and electrochemical perfomance of GO/TiO_2 composite. Catalysis Today, 315, 155-161.

[10] Kamat, P. V. (2010). Graphene-based nanoarchitectures. Anchoring semiconductor and metal nanoparticles on a two-dimensional carbon support. The Journal of Physical Chemistry Letters, 1(2), 520-527.

[11] Zhang, L., Liu, Q., & Sun, Y. (2020). Enhanced photocatalytic activity of $GO-TiO_2$ composites: The role of GO in the nanocomposite. Applied Catalysis B: Environmental, 260, 118195. https://doi.org/10.1016/j.apcatb.2019.118195.

[12] Deshmukh, S. P., Kale, D. P., Kar, S., Shirsath, S. R., Bhanvase, B. A., Saharan, V. K., & Sonawane, S. H. (2020). Ultrasound assisted preparation of rGO/TiO_2 nanocomposite for effective photocatalytic degradation of methylene blue under sunlight. Nano-Structures & Nano-Objects, 21, 100407.

[13] Chong, M. N., Jin, B., Chow, C. W. K., & Saint, C. (2010). Recent developments in photocatalytic water treatment technology: A review. Water Research, 44(10), 2997-3027.

[14] Zafar, M., Imran, S. M., Iqbal, I., Azeem, M., Chaudhary, S., Ahmad, S., & Kim, W. Y. (2024). Graphene-based polymer nanocomposites for energy applications: Recent advancements and future prospects. Results in Physics, 107655.

[15] Li, S., Jiang, H., Yang, K., Zhang, Z., Li, S., Luo, N., ... & Wei, R. (2018). Three-dimensional hierarchical $graphene/TiO_2$ composite as high-performance electrode for supercapacitor. Journal of Alloys and Compounds, 746, 670-676

[16] Wu, X. (2021). Applications of titanium dioxide materials. Titanium Dioxide-Advances and Applications.

[17] Eda, G., & Chhowalla, M. (2009). Graphene-based composite thin films for electronics. Nano Letters, 9(2), 814-818.

[18] Roy, R. K. (2010). A primer on the Taguchi method. Society of manufacturing engineers.

[19] Phadke, M. S. (1989). Quality engineering using robust design. Prentice Hall PTR

[20] HAMZAH, A. A. (2022). Statistical Optimization of Zinc Oxide Nanorod Synthesis for Photocatalytic Degradation of Methylene Blue. Sains Malaysiana, 51(6), 1933-1944.

[21] Reiner-Rozman, C., Hasler, R., Andersson, J., Rodrigues, T., Bozdogan, A., Bintinger, J., & Aspermair, P. (2021). The top performer: Towards optimized parameters for reduced graphene oxide uniformity by spin coating. Micro & Nano Letters, 16(8), 436-442.

[22] Belhadj, W., Timoumi, A., Alamer, F. A., Alsalmi, O. H., & Alamri, S. N. (2021). Experimental study and theoretical modeling of coating-speed-dependent optical properties of TiO2-graphene-oxide thin films. Results in Physics, 30, 104867.

[23] Veeresh Nayak, C., Manjunath Patel, G. C., Ramesh, M. R., Desai, V., & Samanta, S. K. (2020). Analysis and optimization of metal injection moulding process. Materials Forming, Machining and Post Processing, 41-74.

[24] Kumaran, V., Sudhagar, P., Konga, A. K., & Ponniah, G. (2020). Photocatalytic degradation of synthetic organic reactive dye wastewater using $GO-TiO_2$ nanocomposite. Polish Journal of Environmental Studies, 29(2), 1683-1690.

[25] Liang, J., vd. (2012). "Flexible Free-Standing Graphene/SnO2 Nanocomposites Paper for Li-Ion Battery", ACS Appl. Mater. Interfaces, 4, 5742-5748.

[26] Liang, Y., Wang, H., Sanchez Casalongue, H., Chen, Z., & Dai, H. (2010). TiO2 nanocrystals grown on graphene as advanced photocatalytic hybrid materials. Nano Research, 3, 701-705.

[27] Raja, R., vd. (2017). "Effect of TiO2/reduced graphene oxide composite thin film as a blocking layer on the efficiency of dye-sensitized solar cells" Journal of Solid State Electrochemistry, 21(3), 891-903

[28] Joshi, N. C., vd. (2020). Synthesis, adsorptive performances and photo-catalytic activity of graphene oxide/TiO_2 (GO/TiO_2) nanocomposite-based adsorbent. Nanotechnology for Environmental Engineering, 5(3), 1-13.

[29] El Radaf, I. M., & Abdelhameed, R. M. (2018). Surprising performance of graphene oxide/tin dioxide composite thin films. Journal of Alloys and Compounds, 765, 1174-1183.

[30] Songkeaw, P., Onlaor, K., Thiwawong, T., & Tunhoo, B. (2019). Reduced graphene oxide thin film prepared by electrostatic spray deposition technique. Materials Chemistry and Physics, 226, 302-308

[31] He, R., & He, W. (2016). Ultrasonic assisted synthesis of TiO_2–reduced graphene oxide nanocomposites with superior photovoltaic and photocatalytic activities. Ceramics International, 42(5), 5766-5771.

[32] Meral, G., Sarıkaya, M., & Dilipak, H. (2011). Delme işlemlerinde kesme parametrelerinin Taguchi yöntemiyle optimizasyonu. Erciyes Üniversitesi Fen Bilimleri Enstitüsü Fen Bilimleri Dergisi, 27(4), 332-338.

[33] Serencam, H., & Uçurum, M. (2019). Taguchi Deney Tasarımı Kullanılarak Uçucu Kül ile Ni (II) Gideriminde Bazı Adsorpsiyon Parametrelerinin Etkinliğinin İrdelenmesi. Niğde Ömer Halisdemir

Üniversitesi Mühendislik Bilimleri Dergisi, 8(1), 336-344.

[34] Bera, M., Gupta, P., & Maji, P. K. (2018). Facile one-pot synthesis of graphene oxide by sonication assisted mechanochemical approach and its surface chemistry. Journal of nanoscience and nanotechnology, 18(2), 902-912.